Transient Performance Comparison of Switched Doubly-Fed Machine Propulsion Drives

Arijit Banerjee, Steven B. Leeb, and James L. Kirtley
Department of Electrical Engineering and Computer Science, Massachusetts Institute of Technology
Cambridge, Massachusetts, USA
arijit@mit.edu, sbleeb@mit.edu, kirtley@mit.edu

***Abstract*—Switched doubly-fed machines (DFM) offer unique opportunities for creating drives for wide speed range operation with reduced power converter requirements. Seamless performance of the drive is desirable in these applications across the complete speed range, that is, a smooth transition between operating modes and speed ranges. This paper presents a comparison of two switched-DFM drive topologies based on the transient performance specifically around the mode transition speed. Thyristor-based transfer switch operation is compared for the two topologies.**

I. Introduction

Reduced requirements for space and thermal remediation are beneficial or even essential requirements for drives in many applications, especially high power applications for propulsion in ships and locomotives [1]. Stationary applications also benefit from drives that provide useful features like controllable power factor presented to the mains utility without adding to the size or expense of a drive. Generally, these high power variable speed drives (VSD) comprise power converters and electric motors rated on the order of one to several tens of megawatt. Traditionally in these applications, either permanent magnet synchronous [2] or squirrel-cage induction [3] machines have been used. However, these machines have a single electrical port and a single mechanical port for electromechanical energy conversion, thereby requiring a full power converter for variable speed operation.

A doubly-fed machine (DFM) has two accesible electrical ports to control energy conversion that adds extra flexibility for drive design. This flexibility has been widely used in limited speed range application such as in wind power generation to reduce the converter size to a third of the shaft power [4]. In contrast, however, a propulsion application often requires wide operating speed range, including negative drive speed, along with different drive torque requirements. Reconfiguration of the DFM "on-the-fly" offers significant possibilitites for reducing the power processed by the power converter while allowing wide-speed four-quadrant operation of the VSD [5]. These switched-DFM drives have transfer switches that connect one winding (stator) of the DFM to different sources (dc or ac) or short them together based on the rotor speed. A controlled power converter controls electromechanical energy conversion from the other winding (rotor) as shown in Fig. 1.

Configurations of the switched-DFM drives reported in the literature can be broadly classified into two topologies. In the low-speed induction topology (LSI), the DFM stator is shorted at lower drive speed [6], which makes the DFM operate like a cage-induction machine. The rotor power converter not only provides the complete shaft mechanical power but also the total excitation current required by the DFM. In the low-speed synchronous (LSS) topology, the DFM stator is connected to a dc source at lower drive speeds [7], which configures the DFM similar to a wound-field synchronous machine. In this configuration, the rotor power converter provides the complete shaft power while the DFM magnetizing current is shared between the dc source and the rotor power converter to maintain a constant stator flux [8]. At higher drive speeds, in either of the topologies, the DFM stator is connected to the ac source created by an in-situ prime-mover-generator set. During high-speed operation, the rotor power converter controls the slip power to achieve shaft speed control. The transition speed at which the DFM reconfigures between the low-speed mode and the high-speed mode depends on the topology and the required drive torque-speed characteristic.

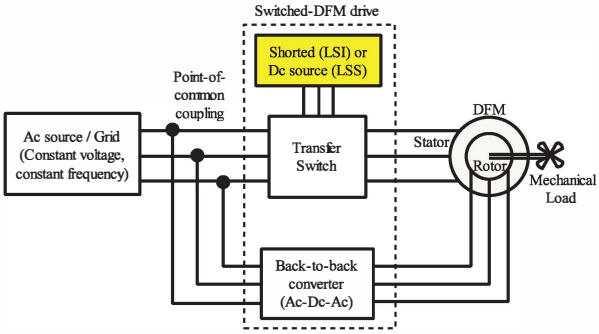

(a)

Figure 1. Generalized switched-DFM drive architecture: At lower shaft speed, the stator is either shorted (LSI) or is connected to a dc source (LSS). At higher shaft speed, the stator is connected to the ac source on-the-fly through the transfer switch.

Seamless performance or "bumpless" switching of the propulsion drive is of prime importance when transitioning between operating modes. The two topologies of the switched-DFM have different mode transition requirements and, therefore, vary in transient performance near the mode transition speed. This paper presents a comparison of the two topologies based on the drive performance near the mode

978-1-4673-6741-7/15/$31.00 ©2015 IEEE

transition speed. The requirements on the DFM during the mode transition are examined. A proposed thyristor-based transfer switch undergoes natural commutation along with a controlled torque at the shaft. The comparison helps in selecting a preferred topology for a given application based on the allowable performance variation of the end application. For example, in ship propulsion, a larger variation in the propeller shaft speed may be tolerable as the propeller and the ship speeds are decoupled through the ship and water inertia. However, in a locomotive the shaft speed directly dictates the vehicle speed and, thereby, a smaller variation from the reference drive torque and speed must be ensured for seamless performance.

II. Dynamic Performance and Control during Mode Transition

The DFM can be thought of as either a synchronous machine or an induction machine during the low-speed mode or as an ac-source-connected doubly-fed induction machine in the high-speed mode. In individual modes, an indirect field-oriented control can enable smooth operation of the drive. The major challenge appears at the mode transition instant when the DFM stator and the rotor power electronic control must be reconfigured "on-the-fly" i.e., while the shaft is turning and producing torque. In this section, first, a generalized DFM transition model with appropriate assumptions is presented. This model can universally represent the mode transition behavior of the DFM irrespective of the stator connection. The requirement for the natural commutation of the thyristors (SCRs) in the transfer switch are next analyzed and compared for the two topologies. Finally, the DFM requirements for a seamless transition are presented for the LSI topology and contrasted with the LSS topology.

A. Generalized stator-flux transition model

Assuming that the rotor current is managed by a high-bandwidth controller and that the drive runs with a relatively low speed controller bandwidth, a closed-loop rotor current-controlled DFM can be modeled using a state-space representation with two state variables, the stator flux magnitude ψ_s and the stator flux angle δ with respect to the stator voltage. The model, independent of the stator connection, is described as:

$$\frac{1}{\omega_b}\frac{d}{dt}\begin{bmatrix}\psi_s\\ \delta\end{bmatrix} = \begin{bmatrix}-\frac{r_s}{x_s}\psi_s + V_{source}\cos\delta\\ \omega_{source} - \frac{1}{\psi_s}V_{source}\sin\delta + \frac{1}{\psi_s^2}r_s\tau\end{bmatrix} + \begin{bmatrix}\frac{r_s x_m}{x_s}\\ 0\end{bmatrix} i_{rd} \quad (1)$$

The parameters of the normalized state-space model are the stator resistance r_s, the stator inductance x_s, and the mutual inductance x_m. The steady-state condition of the stator flux for the individual stator connection is obtained by equating (1) to zero with an appropriate stator source voltage V_{source} and the frequency ω_{source} based on the connection. For example, $(V_{source},\, \omega_{source})$ changes in (1) as $(1,\, 1)$, $(v_{dc},\, 0)$, and $(0,\, 0)$ depending on the stator connection to the ac source, to the dc source (v_{dc}) , or whether the stator windings are shorted together respectively. In the shorted configuration, the stator flux angle δ is relative to the A-phase stator axis as the stator voltage is zero. Assuming a positive drive torque τ, the steady-state condition is graphically represented by SS in the $\psi_s - \delta$ phase plane as shown in Fig. 2 depending on the stator winding connection. When the operating point is perturbed from the steady-state condition, the vector field drives the stator flux trajectory in the phase plane.

When the stator is connected:

1) to the dc source (low-speed mode, LSS topology) - The steady-state is represented by a stationary point in the $\psi_s - \delta$ plane with the ψ_s corresponding to the designed stator flux magnitude (0.72 p.u). The sine of the angle δ depends on the drive torque demand. The operating point SS is inherently a saddle point as observed based on the vector field direction. The operating point is stabilized by proper feedforward terms in the stator flux magnitude controller [8].
2) as a short (low-speed mode, LSI topology) - The DFM operation is represented by a line in the $\psi_s - \delta$ plane with the ψ_s corresponding to the designed stator flux magnitude (0.9 p.u). In this case, the time derivative of δ depends on the drive torque demand. The time derivative of δ corresponds to the slip speed.
3) to the ac source (high-speed mode) - The steady-state is once again represented by a stationary point in the $\psi_s - \delta$ with $\psi_s \simeq 1$ and $\delta \simeq 90°$. The operating point is fairly independent of the drive torque demand for a negligible stator resistance.

A source change-over instantly maps the operating point from one vector field to the other (depending on the pre- and post-transition stator connection) with the identical stator flux magnitude and with initial δ decided by the transition instant. The state trajectory to the final steady-state condition is governed by the vector field and the d-axis current controller command i_{rd}. At the source transition instant, the different constraints on the DFM and on the SCR-based transfer switch are:

1) seamless and controllable drive torque,
2) required rotor voltage within the designed maximum limit to prevent uncontrolled rotor current,
3) minimal stator flux magnitude swing to prevent saturation in the DFM magnetic circuit,
4) natural commutation of the SCRs in the transfer switch, and
5) stator and rotor currents within the respective ratings.

B. Thyristor-based transfer switch operation

The SCR-based transfer switch developed for the LSS topology [9] can be easily adapted for the LSI topology by replacing the dc source with a short as shown in Fig. 3. The transfer switch has twelve thyristors that connect the stator either to the ac source or to the dc source/short depending

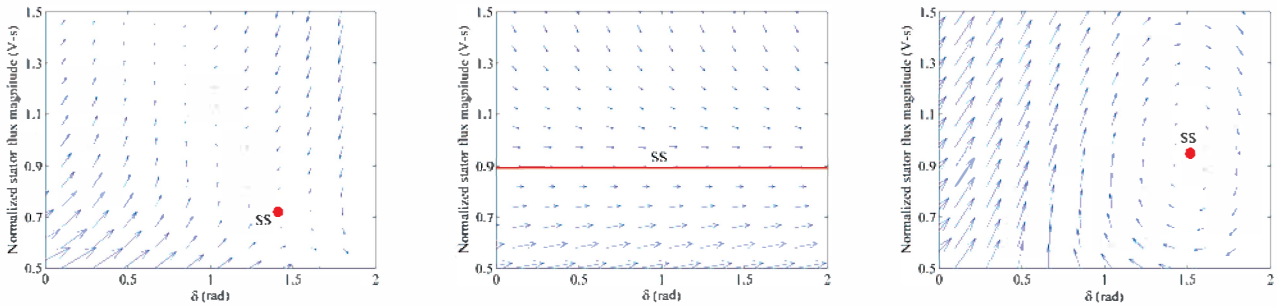

Figure 2. Comparison of the steady-state operating condition SS and the vector field for the individual stator connections. The stator is (a) connected to the dc source, (b) shorted together, or (c) connected to the ac source. A mode transition maps the steady-state condition in the pre-transition vector field as a perturbation in the post-transition vector field.

on the chosen topology. In the LSS topology, assuming the stator is initially connected to the dc source, the current direction in the stator is positive in the A-phase and negative in the B- and C-phases at steady-state. For a simultaneous natural commutation of the outgoing SCRs $T^A_{low,F}$, $T^B_{low,R}$, and $T^C_{low,R}$, the incoming ac source must have a positive A-phase and a negative B- and C-phase voltages with respect to the common ground. This constraint limits the possible natural commutation regions for the outgoing SCRs and requires that the incoming ac voltage vector is within $\pm 30^\circ$ (sector I) as shown in Fig. 4(a) [9].

However, the stator winding carries a bidirectional current at slip frequency during the low-speed operation in the LSI topology. The alternating current polarity opens up possibility of the SCR current commutation in the other sectors as well. The three outgoing SCRs will have simultaneous natural commutation provided that the incoming ac source voltage vector is in the same sector as the stator current vector at the instant of mode transition. The three SCRs on the shorted-side and the three SCRs on the ac source side that participate in the current commutation are determined by the location of the stator current vector. For example, with the stator current vector in sector IV as shown in Fig. 4(b), the stator current from the SCRs $T^A_{low,R}$, $T^B_{low,F}$, and $T^C_{low,F}$ commutate to the SCRs $T^A_{high,R}$, $T^B_{high,F}$, and $T^C_{high,F}$ at the source transition instant.

During the high-speed-to-low-speed mode transition, the stator power factor angle must be between 120° and 240° for simultaneous natural commutation of the outgoing ac source side SCRs. The requirement is identical for both the switched-DFM topologies. The three outgoing SCRs on the ac-source side and the three incoming SCRs on the dc-source side that take part in the current commutation are set by the location of the stator current vector and is given in [9].

C. Low-speed to high-speed mode transition

While the constraint of having the ac voltage vector and the stator current vector within a 60° sector ensures natural commutation of the outgoing SCRs, a correct instant within the

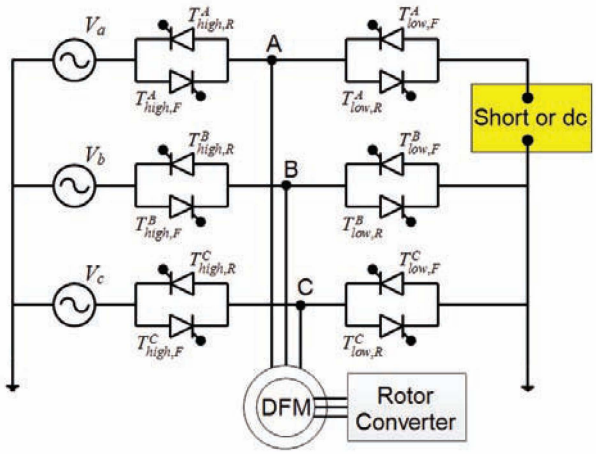

Figure 3. SCR-based transfer switch that connects the stator either to the ac source (in high-speed mode) or to the dc source/short (in low-speed mode).

sector enables the drive torque and the rotor speed controllable and bump-less during the mode transition. The low-speed-to-high-speed mode transition in the LSS topology has been discussed in detail in [9] and will be highlighted here only for the sake of comparison.

Assuming that the DFM is operating in the low-speed mode, the correct instant for a seamless transition is determined by the synchronizer when the d-axis component of the incoming ac source voltage vector matches that of the existing d-axis component of the stator voltage. Additionally, the q-axis component of the incoming ac source voltage vector must be positive at the transition instant [8]. In the LSI topology, the d-axis components of the stator voltage and current are inherently zero by the stator configuration. For any positive drive torque, the stator current vector leads the stator flux vector by 90°. Therefore, the synchronizer requirement can be satisfied when the stator current vector is in phase with the incoming ac voltage vector as shown in Fig. 4(a). For

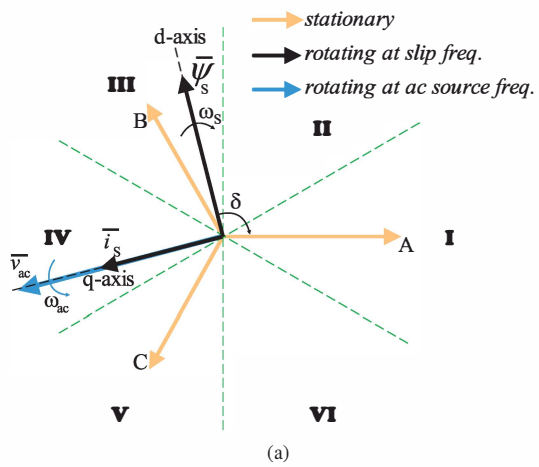

(a)

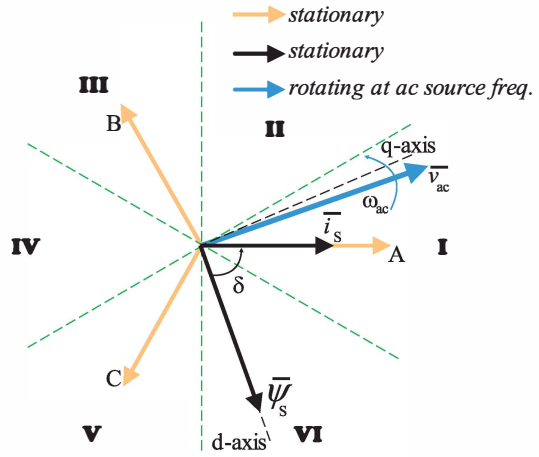

(b)

Figure 4. Space-vector representation of the stator variables for a seamless transition from low-speed to high-speed mode with natural commutation of the SCRs. (a) LSI topology: The stator flux and the stator current vectors rotate at slip frequency in the opposite direction compared to the incoming ac source voltage vector for a positive drive torque demand. (b) LSS topology: The stator flux and the stator current vectors are stationary.

the DFM rotor rotating in the clockwise direction with a positive drive torque, the stator current vector and the stator flux vector rotate in the counter-clockwise direction at slip frequency. The incoming ac voltage vector, however, rotates in the clockwise direction relative to the stator winding axis. The in-phase requirement can be achieved at least once every fundamental ac source cycle and automatically satisfies the constraint for natural commutation of the outgoing SCRs for any positive drive torque. In general, the low-speed-to-high-speed mode transition inherently involves a positive drive torque requirement at the shaft.

For a low-speed-to-high-speed mode transition in the LSS topology, the incoming ac source voltage vector need not necessarily be in phase with the stator current at the correct transition instant as determined by the synchronizer because the stator contributes to the DFM magnetizing current. In the

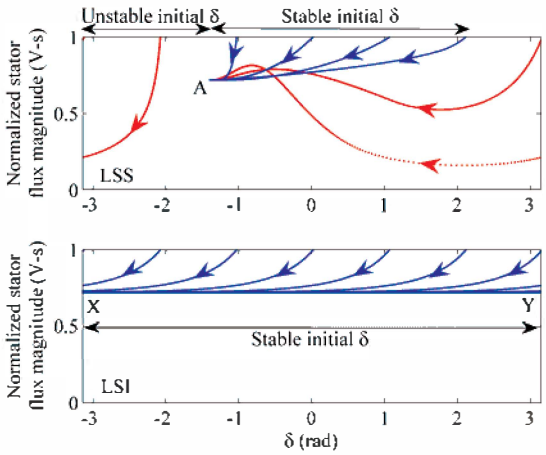

Figure 5. Stator flux trajectory comparison for a high-speed to low-speed mode transition. Top: LSS topology: The initial δ must be within specific limits to ensure a controllable torque during mode transition Bottom: LSI topology: The mode transition is stable and seamless for all initial δ.

LSS topology, the stator current and the stator flux vectors are stationary relative to the stator winding axis. The constraints of natural commutation of the outgoing SCRs and the correct instant of transition for seamless transition at the DFM shaft are satisfied for high drive torque demand as shown in Fig. 4(b). At lower drive torque demand with the angle δ relatively small, the requirement for natural commutation of the outgoing SCRs is given priority and the DFM stator is switched at the boundary of sector I. Not meeting the optimum instant of transition from the DFM perspective leads to additional perturbation in the stator flux during source change-over. Extra care is needed for the drive to operate with controllable current without being voltage limited on the rotor converter. A smoother transition can still be achieved with proper damping using rotor d-axis current controller after the source transition. The boundary of the light load torque is given in [9].

D. High-speed to low-speed mode transition

With the DFM initially operating in the high-speed mode, the constraint of the stator power factor angle for the natural commutation of the outgoing SCRs can be satisfied by a reverse active power flow and with an appropriate stator reactive power control using the rotor converter command. The stator flux trajectory at the instant of the high-speed-to-low-speed mode transition is compared for the two topologies in Fig. 5. Assuming the initial normalized stator flux magnitude is unity and the final stator flux magnitude for the low-speed mode is 0.72, the stator flux trajectory follows a different path based on the transition instant set by the initial angle δ. For the LSS configuration, the initial δ has to be within zero and 90° for a stable high-speed-to-low-speed mode transition [9]. Beyond this range of δ, the stator flux magnitude collapses below the target stator flux magnitude (represented by A in Fig. 5), which can lead to an uncontrolled shaft torque disturbance. The required constraint for the initial δ is ensured

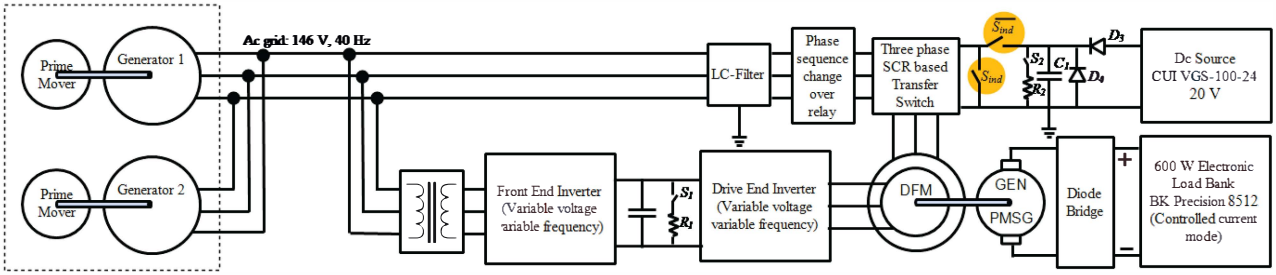

Figure 6. Experimental setup to compare the transient performance of the two topologies. The ac source is made from two synchronous generators that can supply 700 W individually while the switched-DFM drive consumes 80% of the generated active power at rated operating condition.

by switching from the ac to the dc source when the ac source voltage vector is within zero and 90° with respect to the stator A-phase axis. The final δ is negative due to the negative drive torque demand as applicable during braking.

However, the ac-source-to-shorted-stator configuration change-over is always stable in the LSI topology, irrespective of the initial δ set by the mode transition instant as shown in Fig. 5. This implies that the ac source voltage vector can be anywhere relative to the stator winding during high-speed-to-low-speed mode transition. The direction of the state trajectory is opposite to that of the vector field shown in Fig. 2(b) due to the negative drive torque demand during braking. After the transition, the steady-state condition corresponds to the line XY in Fig. 5.

III. Experimental Results

The experimental setup used to compare the transient performance of the two topologies of the switched-DFM drive is shown in Fig. 6. The 146 V (line-to-line, rms), 40 Hz ac source is created using two parallel-operated synchronous generators that provide power to the switched-DFM drive. The stator of the DFM is connected to a SCR-based transfer switch that can toggle the stator connection to the ac source during high-speed mode operation. During low-speed mode operation the stator is connected either to a separate dc source in the LSS topology or is shorted together in the LSI topology using the switch S_{ind}. The rotor of the DFM is connected to the ac grid using a back-to-back converter configuration using two Texas Instruments High Voltage Motor Control & PFC Developer's Kits. The grid voltage and frequency has been chosen such that the off-the-shelf 1 HP, 220V/150V, 4 pole, 1800 rpm DFM operates within the rated speed at rated stator flux magnitude in high-speed operating mode. The parameters of the DFM are given in [5]. The DFM is connected to a load generator, which can operate with different load torque profiles with respect to the speed. The mode transition is determined by a hysteresis comparator that compares the rotor speed to the high ω_2 and low threshold ω_1 setpoints. For the LSI topology, $\omega_{1,si}$ is 597 rpm and $\omega_{2,si}$ is 633 rpm. For the LSS topology, $\omega_{1,ss}$ is 757 rpm and $\omega_{2,ss}$ is 793 rpm respectively.

In the LSI topology, the stator currents and the ac source voltages during mode transitions are shown in Fig. 7(a) and (b) respectively. The ac source voltage follows a ABC sequence. At the low-speed-to-high-speed mode transition instant in Fig.7(a), the polarity of the stator currents match the polarity of the respective ac source phase voltages implying a natural commutation of the outgoing SCRs. The phase sequence of the stator current changes from ACB to ABC at the transition instant. At the high-speed-to-low-speed mode transition instant in Fig. 7(b), the polarity of the stator current is opposite to the polarity of the ac source phase voltage due to the reverse active power flow and a stator reactive power control using the rotor converter. The phase sequence of the stator current after and before the transition remains the same in this case.

The most critical transient performance comparison for the two topologies is the drive behavior near the mode transition speed. The drive response for an alternating reference speed command encompassing the mode transition speed is compared in Fig. 8. With an identical constant load torque at the shaft, both the topologies speed response is identical. A higher overshoot during high-speed-to-low-speed mode transition is due to the requirement of the reverse power flow to achieve the natural commutation of the outgoing SCRs.

In the next experiment, the reference speed is set midway between the lower and higher threshold of the hysteresis comparator that commands the mode transition. An oscillating load of 18% to 55% of the full load makes the perturbation in the rotor speed such that the DFM drive operates in the low- and high-speed modes alternatively. The LSS topology exhibits a larger swing in the rotor speed due to the load disturbance as it has more constraints to satisfy for proper mode transition.

IV. Conclusions

This paper presents a comparison of transient performances of the two switched-DFM drive topologies. Different considerations and constraints are highlighted to ensure a seamless transition at the shaft for the individual topologies. Analysis and experimental results shows a smoother performance of the LSI topology compared to the LSS topology in and around the mode transition speed due to relaxed constraints for the source change-over. The seamless performance of the switched-DFM drive can result in a compact and efficient drive with reduced power converter size enabling wide speed range operation suitable for many high power applications.

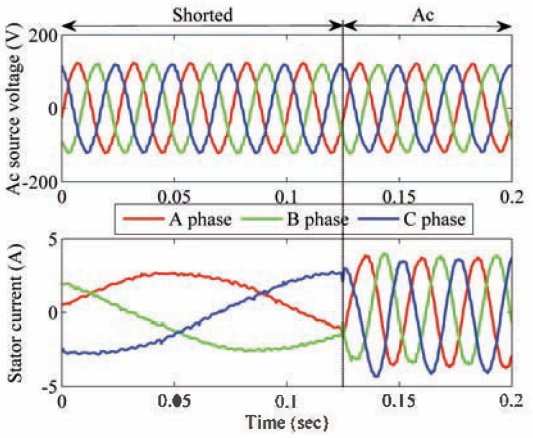

(a)

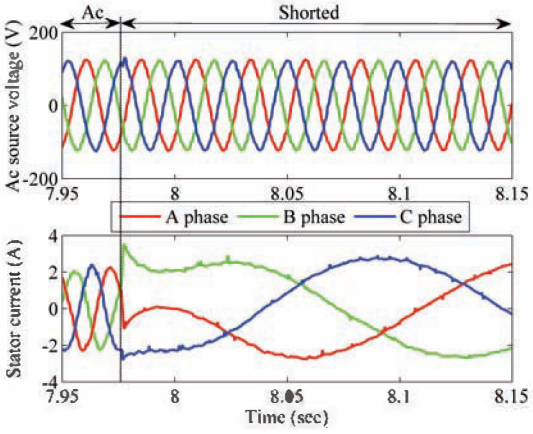

(b)

Figure 7. Experimental results: Ac source phase voltages and the stator currents during the mode transition instances in the LSI topology. (a) The stator current is at slip frequency when shorted and transitions to grid frequency at the low-speed-to-high-speed mode transition instant. (b) The stator current is initially at grid frequency and changes over to slip frequency during high-speed-to-1ow-speed mode transition.

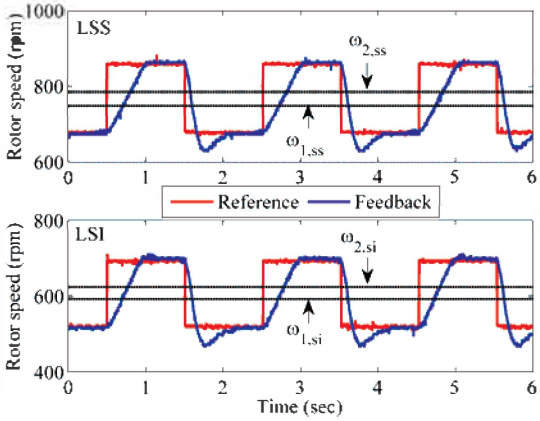

Figure 8. Comparison of the switched-DFM drive topologies based on the speed response to an alternating reference speed with a constant load torque around the mode transition speed. The responses of the two topologies are identical.

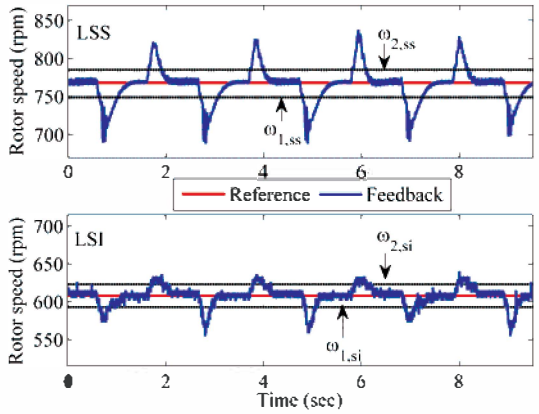

Figure 9. Comparison of the switched-DFM drive speed response to a constant reference speed with a load torque variation between 18% to 55% of full-load torque. The speed perturbation enforces the drive to operate in the two modes alternatively. The LSI topology exhibits a smaller swing in the rotor speed during the mode transition due to the relaxed transition requirements.

ACKNOWLEDGMENT

This research was performed with support from the Kuwait Foundation for the Advancement of Sciences (KFAS) through the Kuwait-MIT Center for Natural Resources and the Environment (CNRE), the Skoltech-MIT SDP Program, and The Grainger Foundation.

REFERENCES

[1] S. Kouro, J. Rodriguez, B. Wu, S. Bernet, and M. Perez, "Powering the future of industry: High-power adjustable speed drive topologies," *Industry Applications Magazine, IEEE*, vol. 18, no. 4, pp. 26–39, July 2012.

[2] L. Parsa and H. Toliyat, "Five-phase permanent magnet motor drives for ship propulsion applications," in *Electric Ship Technologies Symposium, 2005 IEEE*, July 2005, pp. 371–378.

[3] C. Lewis, "The advanced induction motor," in *Power Engineering Society Summer Meeting, 2002 IEEE*, vol. 1, July 2002, pp. 250–253 vol.1.

[4] S. Muller, M. Deicke, and R. De Doncker, "Doubly fed induction generator systems for wind turbines," *Industry Applications Magazine, IEEE*, vol. 8, no. 3, pp. 26–33, May 2002.

[5] A. Banerjee, M. Tomovich, S. Leeb, and J. Kirtley, "Power converter sizing for a switched doubly fed machine propulsion drive," *Industry Applications, IEEE Transactions on*, vol. 51, no. 1, pp. 248–258, Jan 2015.

[6] L. Morel, H. Godfroid, A. Mirzaian, and J.-M. Kauffmann, "Double-fed induction machine: converter optimisation and field oriented control without position sensor," *Electric Power Applications, IEE Proceedings -*, vol. 145, no. 4, pp. 360–368, Jul 1998.

[7] S. B. Leeb, J. L. Kirtley, W. Wichakool, Z. Remscrim, C. N. Tidd, J. A. Goshorn, K. Thomas, R. W. Cox, and R. Chaney, "How much dc power is necessary?" *Naval Engineers Journal*, vol. 122, no. 2, pp. 79–92, 2010.

[8] A. Banerjee, M. Tomovich, S. Leeb, and J. Kirtley, "Control architecture for a switched doubly fed machine propulsion drive," *Industry Applications, IEEE Transactions on*, vol. 51, no. 2, pp. 1538–1550, March 2015.

[9] A. Banerjee, A. Chang, K. Surakitbovorn, S. Leeb, and J. Kirtley, "Bumpless automatic transfer for a switched doubly-fed machine propulsion drive," *Industry Applications, IEEE Transactions on*, vol. PP, no. 99, pp. 1–1, 2015.